



Consideration of Temperature Factors when Designing Butterfly Check Valves for Hazardous Production Facilities

Julia Soboleva ¹, Abdulmejid Kerimov ¹, Abas Lampezhev ^{1*}

¹ *Institute of Design and Technology Informatics, Russian Academy of Sciences, Moscow, Russian Federation.*

Received 01 July 2023; Revised 04 December 2023; Accepted 15 December 2023; Published 26 December 2023

Abstract

The safety of hazardous production facilities is directly related to the reliability of pipeline systems, which must be ensured regardless of environmental conditions. Accidents on pipeline sections can have catastrophic consequences associated with damage to human health and the environment. Damage to the metal of pipeline elements during operation due to internal corrosion occurring under the influence of the working fluid is one of the main reasons for failure. This study aims to develop an improved butterfly check valve (BCV), which is a pipeline element. For this purpose, various structural materials used in the production of check valves were analyzed, and the changes in their mechanical properties under the influence of temperature were also considered. Based on this material, a butterfly check valve was developed. The stress-strain state of the developed structure was assessed using the finite element method (FEM). Strains, stresses, and displacements were calculated to evaluate valve performance. These calculations are necessary to determine the most loaded elements of the BCV at the maximum and minimum ambient temperatures. The following conclusions were obtained: X6CrNiTi18-10 stainless steel grade is the most suitable material for piping systems transporting liquids in production facilities. On the basis of the simulation results, the values of equivalent stresses, maximum strains, and displacements were obtained. The research results confirmed the performance of the improved design, the unhindered motion of the working fluid in the working direction, and the convenient connection to horizontal and vertical sections of the pipeline.

Keywords: Pipeline System; Shut-off Valves; Butterfly Check Valve; Mathematical Modeling; Finite Element Method.

1. Introduction

The pipeline system, which ensures the operation of most communication systems, nuclear and thermal plants, electrical systems, etc., is one of the important parts of production facilities [1–3]. The industrial safety of hazardous production facilities is directly related to the efficient operation of the pipeline, which can be performed around the clock, regardless of the climatic state of the environment [4, 5]. Failures in such systems can cause economic and environmental damage, such as environmental pollution, the death of flora and fauna, etc. [6–8]. Therefore, special requirements are imposed on them, the most important of which is to ensure the reliable and safe operation of pipelines [9]. To do this, a non-destructive method is used to assess the technical condition of the pipeline system, including an automated assessment, the main tasks of which are to identify damage and structural defects that could cause an accident [10–12].

* Corresponding author: abas.lampezhev@mail.ru

<http://dx.doi.org/10.28991/CEJ-SP2023-09-020>



© 2023 by the authors. Licensee C.E.J, Tehran, Iran. This article is an open access article distributed under the terms and conditions of the Creative Commons Attribution (CC-BY) license (<http://creativecommons.org/licenses/by/4.0/>).

Any pipeline includes parts related to shut-off and control valves, control measuring instruments, fasteners, anti-corrosion elements, and other structural components [13, 14]. Pipeline fittings are designed to control the working fluid flows: distribution, regulation, shutdown, and mixing. Working fluids can be liquid, gaseous, powdery, or suspension, etc. [15–17]. Industrial fittings are designed to operate with corrosive, aggressive, or toxic media, vapors, and high-pressure media.

Valves are divided into shut-off, control, safety, protective, phase separation, and distribution [18–20]. Butterfly check valves ensure fluid motion in one direction and prevent it in the opposite direction [21, 22]. When the flow motion changes in the opposite direction, the valve automatically closes. A sufficient number of pipeline fittings have been developed. Collison, Engle, and Hodny developed a valve in which the body parts were made by casting and stamping, in particular a wedge valve consisting of a cast cover connected to a body in which a valve assembly is located, controlled by a spindle sealed relative to the cover [23]. The destruction of the cover and body in the event of working fluid freezing and a decrease in ambient temperature is a disadvantage of this design.

Bazarov et al. [24] developed wedge valve fittings containing a cover connected to a body that houses a valve assembly controlled by a spindle sealed against the cover. However, in this design, the weld seam that welds the bottom to the body is destroyed if the pressure inside the valve increases above the critical value when the working fluid freezes due to a change in ambient temperature. Thus, the valve fails and loses its functionality. Thus, the issue of developing pipeline fittings that can withstand changes in ambient temperature, leading to freezing and thawing in internal cavities without loss of performance, becomes relevant. When designing BCVs, it is necessary to consider the materials from which they are made, since many system failures are associated with their corrosive wear [25–27]. The purpose of this research is to create pipeline fittings that can withstand repeated changes in ambient temperature.

2. Materials for the Pipeline Fittings

The materials used in the manufacture of pipeline fittings are divided into groups according to their purpose: vessel, sealing, gasket, leak-proofing, and lubricating materials. In this study, only vessel materials that require high strength, corrosion resistance, and manufacturability will be considered. Owing to its good casting quality, ductility, and ease of processing, steel is one of the most common structural materials. The following steel grades are used to manufacture pipeline elements for hazardous production facilities: C22, X6CrNiTi18-10, P275N, C25N, 24CrMoV5-5, 24CrMo5, and X22CrMoV12-1 (DIN). Among the presented steels, C22 and X6CrNiTi18-10 are the most commonly used. C22 stainless steel (see Table 1). These steel grades are used in industry for the production of machine parts and mechanisms, such as shafts, axles, gears, levers, etc.

Table 1. Chemical composition of C22 stainless steel in (%) [28]

C	Si	Mn	Ni	S	P	Cr	Mo	Ni	Fe
0.17–0.24	<0.4	0.4–0.7	<0.4	<0.045	<0.045	<0.4	<0.1	<0.4	the remainder

Silicon, which is part of the alloy, removes particles of hydrogen, oxygen, and nitrogen from the composition, thereby increasing the strength of the steel. Manganese provides sulfur removal and has a positive effect on the surface quality.

X6CrNiTi18-10 stainless steel. Steels of this type are the predominant material in the areas of refrigeration and cryogenic technology because of their high ductility, viscosity at low temperatures, and high corrosion resistance (see Table 2).

Table 2. Chemical composition of X6CrNiTi18-10 stainless steel in (%) [28]

C	Si	Mn	Ni	S	P	Cr	Ni	Fe
<0.08	<1	<2	9–12	0.015	<0.045	17–19	9–12	the remainder

The presence of titanium in chromium-nickel steels eliminates the tendency for corrosion when heated. Chrome provides corrosion resistance and increases the cold brittleness threshold. Alloying with nickel increases ductility and hardenability, reduces grain size, and decreases the concentration of impurities in dislocations. Austenitic chromium-nickel steel grades also have high resistance to solutions of organic acids, which enables the manufactured fittings to work in aggressive environments.

3. Material and Methods

3.1. Theoretical and Analytical Study of Changes in the Properties of Metals During Operation

The research process is shown in Figure 1.

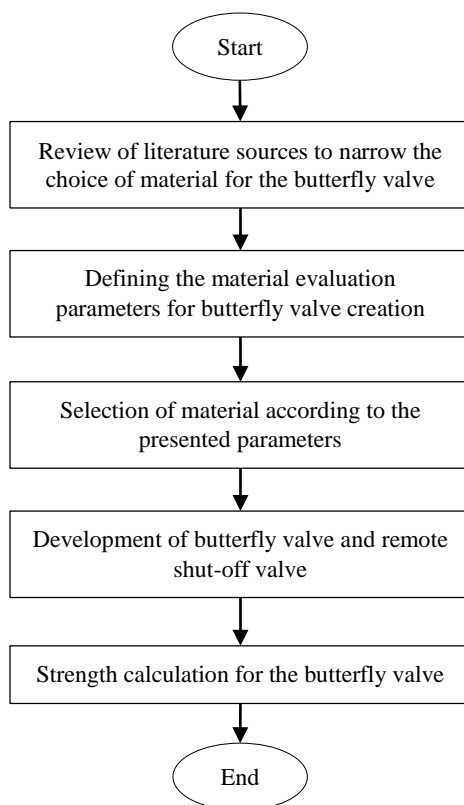


Figure 1. Flowchart for studying changes in the properties of metals during BCV operation

The long-term use of any metalware results in the deterioration of its physical parameters; therefore, even under the influence of design loads, it is often possible to observe its deformation. Decreased resistance to physical damage is caused by increased cognitive stress, the metal aging process, and thinning of the walls, which usually occurs due to rusting. The main factor in the premature destruction of a pipeline is its prolonged contact with an external corrosive medium (stress corrosion), which is influenced by parameters such as pressure, pH level of the corrosive medium, metal mechanical properties, and structure. That is why it is essential to study the chemical composition and level of metal resistance to corrosion.

Numerous processes that naturally occur in metal piping systems negatively affect the physical characteristics of the materials used in these systems during their long-term operation. Due to the fact that pipe microcracking is caused by local changes in the structure of metals, some specialized studies have been conducted to assess the level of long-term impact on the resistance to destruction of metals, which identify the pronounced tendency of the metal to deformation, the characteristics of resistance to fracture formation, resistance to fracture nucleation and diffusion, and others.

However, precisely the nature of the occurrence of the effects under consideration is of particular interest, which can be described using a sample of P275N steel pipe. In this case, the values of temporary tensile strength vary in the range of $563 \pm 62 \text{ N/mm}^2$, which corresponds to the ISO 5952-83 standard for this material. Studies performed under various bends of the assessed product demonstrated deterioration in the parameters of resistance to physical damage. Thus, twenty-five years of operation showed a decrease in impact strength of 18–19%. In this case, KCU decreased from 59.4 to 49.7 J/cm² at -37–39 °C and from 59 to 48.4 J/cm² at +18–19 °C.

Upon completion of thirty years of operation of metal pipes, the temperature limits of cold brittleness move into the category of positive temperatures; therefore, the process of fracture diffusion with increasing temperatures is described by unstable algorithms (see Figure 2).

Forty years of operation reduces the level of fracture toughness from 44 to 31.9 MPa.m^{1/2}. The values of the largest openings of COD fractures are reduced by 1.35–1.41 times, and metals demonstrate increased sensitivity to cognitive stress.

Simultaneously, the diffusion of permanent fractures will also be determined primarily by the duration of the operation. Thus, P275N steel pipes are characterized by minimal diffusion of permanent fractures (strain indicators $K = 59 \dots 61 \text{ MPa.m}^{1/2}$). With an increase in the duration of pipe operation, the diffusion rates of permanent fractures increase, and with forty to forty-five years of operation, they can reach $(79 \dots 81) \times 10^{-4}$ millimeters per minute.

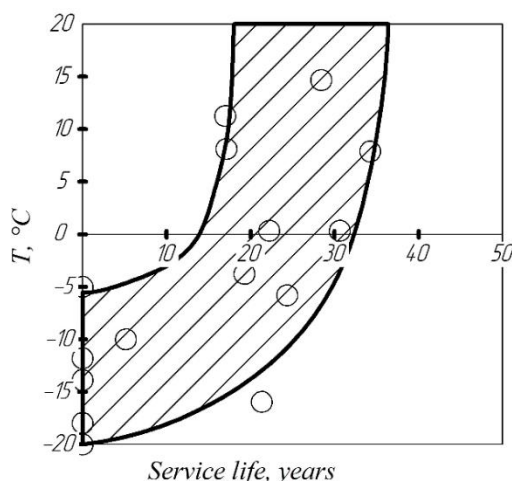


Figure 2. Degree of long-term operation impact on the temperatures of transitions to brittle states of P275N metal pipe

3.2. Study of the Influence of Temperature on the Properties of the Material from which BCV is Made

The fatigue endurance of steel is conditioned by the totality of its mechanical and technological properties, which depend on its chemical composition and structural state. Strength and ductility are the main mechanical properties. Strength is determined by the ability of a material to resist the applied force without breaking. Ductility is the ability of a material to deform irreversibly without breaking under a load and to retain these changes after the load is removed.

In general, the physical properties of a material are characterized by inconstancy, and its main parameters are determined by temperature, deformation rate, and others.

To assess the effect of temperature on steel products, several coefficients must be used:

- **Strength factor:**

- The strength limit is expressed by the value of σ_u .
- Comparative inconstancy is expressed as $\sigma_{0.2}$.

- **Ductility criteria:**

- Relative elongation δ is the ratio of the increment in the calculated length of the sample after rupture to its initial calculated length.
- Relative narrowing ψ is the ratio of the difference between the initial and minimum cross-sectional areas of the sample after rupture to its initial cross-sectional area.

The parameters δ and ψ can be determined from the ratio of flow stress σ_s , fracture stress σ_f and strain hardening. Material ductility increases with increasing temperature because elevated temperatures facilitate the movement of dislocations in solids. When testing stainless steel, for example, during compression or tensile testing, increasing temperature has a strong impact on its mechanical properties. Figure 3 shows the change in the properties of C22 steel with an increase in temperature to 600°C.

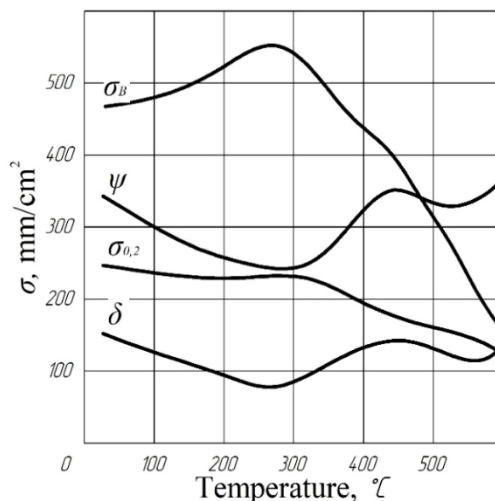


Figure 3. Degree of temperature impact on some physical properties of the C22 pipe

Thus, the curves describing inconstancy in the range of up to 300°C indicate a characteristic area of inconstancy; however, with increasing temperatures, the inconstancy decreases. Technological annealing (from 195 to 298°C) improves strength indicators and simultaneous deterioration in metal ductility. It was shown that the elastic moduli of the metal decrease with increasing temperature. Steel is strengthened during cold plastic deformation, but at the same time, steel ductility and impact strength decrease (natural aging). As the temperature increases, this process accelerates; impact strength can reach approximately 12% of the original value (artificial aging). Tables 3 and 4 indicate the mechanical characteristics of C22 and X6CrNiTi18-10 stainless steel grades in the temperature range from 20 to 500°C.

Table 3. Mechanical properties of C22 stainless steel grade at different temperatures

Test temperature, °C	$\sigma_{0.2}$, MPa	σ_u , MPa	δ , %	ψ , %
20	280	430	34	67
200	230	405	28	67
300	170	415	29	64
400	150	340	39	81
500	140	245	40	86

Table 4. Mechanical properties of X6CrNiTi18-10 stainless steel grade at various test temperatures

Test temperature, °C	$\sigma_{0.2}$, MPa	σ_u , MPa	δ , %	ψ , %
20	275	610	41	63
300	200	450	31	65
400	175	440	31	65
500	175	440	29	65

The following notation is used in Tables 3 and 4: $\sigma_{0.2}$ is the conditional yield strength, MPa; σ_u – ultimate tensile strength (tensile strength), MPa; δ – tensile strain, %; ψ – constriction at break, %. Therefore, it makes sense to study the degree of temperature impact on the limiting values of long-term rupture strength (since the stress caused by the temperature impact simply destroys the main components of the material over a certain period of time).

At the same time, the strength properties are determined by stable bonds between neighboring atoms due to their natural bonding. Thus, deformation occurs because of a violation of the interatomic correlation under the temperature impact. Simultaneously, a decrease in strength was observed at cryotemperatures. Moreover, due to the impact of energy bursts in metals, some centers (of components) may be underloaded. Furthermore, the stable mutual connection of the main molecular regions with each other causes some new vacancies.

When stress is applied to the metal, vacancies and dislocations move and accumulate along grain boundaries and near defects and microdefects in the structure. Because of the large accumulation of vacancies and dislocations, microcracks are formed, which subsequently become stress concentrations, resulting in destruction.

3.3. Development of the Butterfly Check Valve

As part of this work, a butterfly check valve was developed consisting of the following components: Valve Body; Cover; Disk; Seat; Lever. This design ensures the working fluid motion in a given direction and prevents it from moving in the opposite direction; it can connect to the horizontal and vertical sections of the pipeline (see Figure 4).

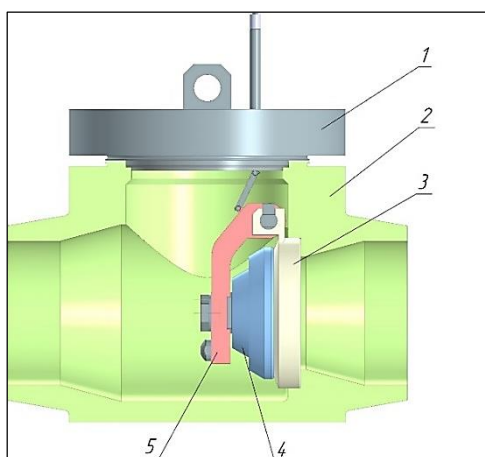


Figure 4. Valve design: 1 – cover, 2 – body, 3 – seat, 4 – disk, 5 – lever

The T-shaped body is manufactured using casting followed by milling. The monolithic design provides a high level of tightness and has a technological hole in the upper part through which the main structural elements are installed. Repairs and replacements of internal parts are carried out without dismantling the valve from the pipeline. The disk acts as a damper, which ensures a hermetically sealed shutoff of the flow. When moving in the working direction, the fluid lifts the damper; when flowing in the opposite direction, the damper is pressed tightly under the influence of the fluid.

The seat is installed in the groove of the body and ensures a tight fit of the disc. The L-shaped lever is designed to drive the shut-off valve. It is attached to the seat via a shaft and ensures the opening and closing of the shut-off element along the working path. The lever design provides the force on the disk necessary to tightly fit the working surface of the disk to the seat and ensure a complete, sealed shutoff of the transported fluid flow.

The valve cover is designed to ensure the tightness of the butterfly check valve and protect the structure from foreign bodies entering. The cover design provides a technological hole for mounting a remote indicator of the shut-off element's position. To install the indicator, a metal tube is welded to the upper surface of the cover, in which the shut-off element target of the butterfly check valve moves freely (see Figure 5).

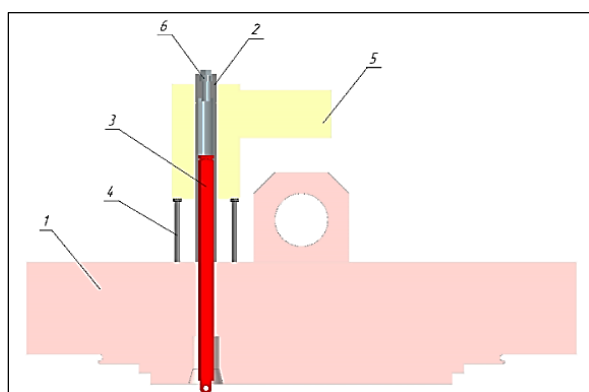


Figure 5. Design of the remote indicator of the shut-off element position: 1 – cover, 2 – bushing, 3 – target, 4 – studs of the remote indicator of the shut-off roller position, 5 – remote indicator of the shut-off element position, 6 – plug

Strains, stresses, and displacements were calculated to assess the performance of the developed structure.

3.4. Strength Calculation for Butterfly Check Valve Design

To analyze the strength of a structure, its stress–strain state under given loading conditions is considered. The stress–strain relationship is established by Hooke’s law, according to which stresses at a point are directly proportional to strains. In addition, theoretical ductility can be determined by a technique that relies on the following basic elastic solutions:

$$\sigma_{ij}^{(m)} = C \left(Y_2(\varepsilon^{(m-1)}) \right)_{ijkl} \varepsilon_{kl}^{(m)}, \tag{1}$$

here $\sigma_{ij}^{(m)}$ and $\varepsilon_{kl}^{(m)}$ are stress and strain affinors at the m -th steps of the current process, $Y_2(\varepsilon)$ – second invariant of the deformation tensor, $C(Y_2(\varepsilon^{(m-1)}))$ is the fourth rank tensor.

When selecting the repetition rate, the condition under which the specified value Δ is achieved, which is the current voltage offset, should be determined as follows:

$$\max_{x_k \in V} \frac{\sum_{i,j} |\sigma_{ij}^{(m)}(x_k) - \sigma_{ij}^{(m-1)}(x_k)|}{\sum_{i,j} |\sigma_{ij}^{(m-1)}(x_k)|} < \Delta. \tag{2}$$

Representation in the form of linear problems:

$$\begin{cases} \sigma_{ij,j}^{(m)} = 0 \text{ in } V; \\ \sigma_{ij}^{(m)} = C \left(Y_2(\varepsilon^{(m)}) \right)_{ijkl} \varepsilon_{kl}^{(m)} \text{ in } V \cup \Sigma; \\ \varepsilon_{kl}^{(m)} = \frac{1}{2} (u_{i,j}^{(m)} + u_{j,i}^{(m)}) \text{ in } V; \\ u_i^{(m)} = u_i^e \text{ on } \Sigma_{u1}; u_i^{(m)} = 0 \text{ on } \Sigma_{u2}; \\ \sigma_{ij}^{(m)} n_j = 0 \text{ on } \Sigma_\sigma, \end{cases} \tag{3}$$

here σ_{ij} , and ε_{kl} are the current Cartesian components of each strain and stress affnor; u_i are components of the displacement gradient; $F_{ij}(\varepsilon_{kl})$ are nonlinear dependencies that describe the simulation of ductility; $u_{j,i}$ are private

compilations; u_i^e – established displacements for increment Σ_{u1} of body surfaces; for this case, we will express surface fragments Σ_{u2} as clearly fixed.

Numerical solutions of problem (3) at any repetition are based on finite element methods. Thus, the variational formulation of condition (3) can be expressed as follows:

$$\int_V \delta \varepsilon^{(m)T} \sigma^{(m)} dV = \int_{\partial V} \delta u^{(m)T} S^{(m)} d\Sigma, \tag{4}$$

where $S^{(m)} = [S_1^m, S_2^m, S_3^m]^T$ – coordinate column of the surface force vector.

In this case, a number of coordinate columns are used for the components of the displacement gradient:

$$\begin{aligned} u^{(m)} &= [u_1^{(m)}, u_2^{(m)}, u_3^{(m)}]^T; \\ \sigma^{(m)} &= [\sigma_{11}^{(m)}, \sigma_{22}^{(m)}, \sigma_{33}^{(m)}, \sigma_{12}^{(m)}, \sigma_{23}^{(m)}, \sigma_{31}^{(m)}]^T; \\ \varepsilon^{(m)} &= [\varepsilon_{11}^{(m)}, \varepsilon_{22}^{(m)}, \varepsilon_{33}^{(m)}, \varepsilon_{12}^{(m)}, \varepsilon_{23}^{(m)}, \varepsilon_{13}^{(m)}]^T \end{aligned} \tag{5}$$

Therefore, calculations of certain designs of check valves should be based on identifying the most loaded sections, which are loaded differently.

The structural state of the valve can be assessed by the stress–strain states of the BCV components, due to modeling using the finite element method, considering the highest and lowest temperatures. Assessment is performed in the plane of the finite-element program product slice by automatically splitting the sample into a number of finite elements. This simplified assessment makes it possible to identify the most loaded sections and analyze the degree of compliance with current conditions, etc. During the calculation of stress–strain states, the valve simulation was simplified by removing minor, lightly loaded, and small components that did not affect the calculation result. The created valve simulation is shown in Figure 6



Figure 6. Simulation model of the DN250 valve

When solving a numerical simulation problem, a mesh is created with large cells on large-area planes and with tapering cells toward the holes to reduce calculation time and decrease the load on the system. Large surfaces were divided along mutually perpendicular planes, after which the size of the elements on the surfaces and edges was indicated. Such a grid makes it possible to generalize the results over a large area while maximally considering the deformation of the most loaded areas of the structure (Figure 7). The sensitivity of the numerical model was another essential factor. To achieve maximum model sensitivity, the number of finite elements was varied until a convergence value of less than 5% was achieved.

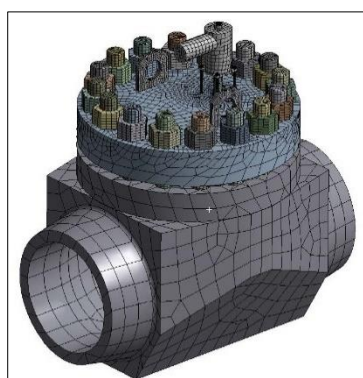


Figure 7. Optimized finite-element mesh in the DN250 butterfly check valve

When modeling the stress–strain state, the following assumptions were made:

- Materials are solid and homogeneous;
- The chemical composition and state of aggregation of the materials are unchanged during the calculation process;
- There are no heating processes as a result of deformation;
- There are no extraneous external impacts on the base;
- The loads are constant, applied in one direction, and their values do not depend on time.

To conduct a finite-element analysis of the stress–strain state, 08X18H10T material, which is an analog of X6CrNiTi18-10, was assigned the structural element of the valve.

4. Research Results

The simulation results include the maximum stresses and strains of the valve structural elements loaded in accordance with the design diagram (see Table 5).

Table 5. Results of the structure strength calculation in the closed state

Calculation condition	Parameters	Maximum equivalent stresses	Maximum strains	Maximum displacements
		σ_{max} , MPa	Δ_{max} , %	δ_{max} , mm
Maximum ambient temperature 45°C	Closed	257.91	0.130	0.17
	Opened	337.62	0.169	0.57
Minimum ambient temperature -5°C	Closed	269.70	0.136	0.14
	Opened	303.12	0.156	0.64

Figure 8 shows graphical representations of the distribution of equivalent stresses in the volumes of the valve models at the maximum permissible temperature (45°C).

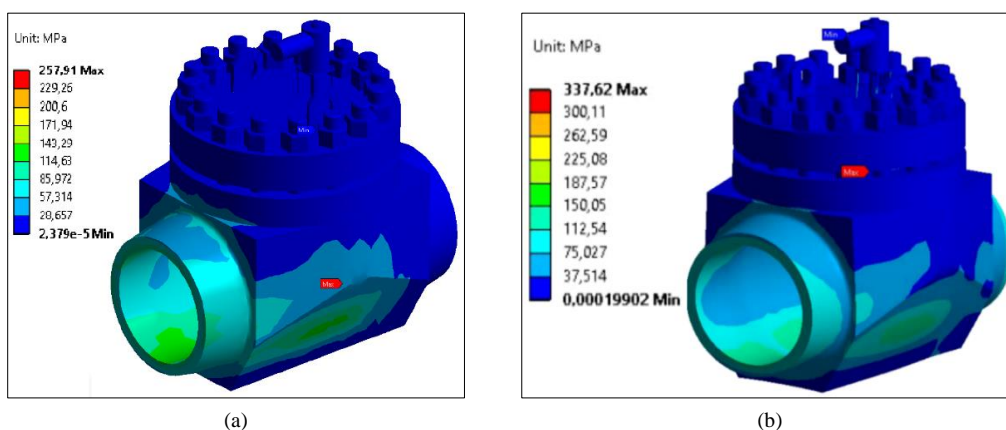


Figure 8. Distribution of equivalent stresses in the volume of the DN250 butterfly check valve at the maximum permissible temperature: a – cover closed; b – cover opened

Figure 9 shows graphical representations of the distribution of equivalent stresses in the volumes of the valve models at the minimum permissible temperature (-5°C).

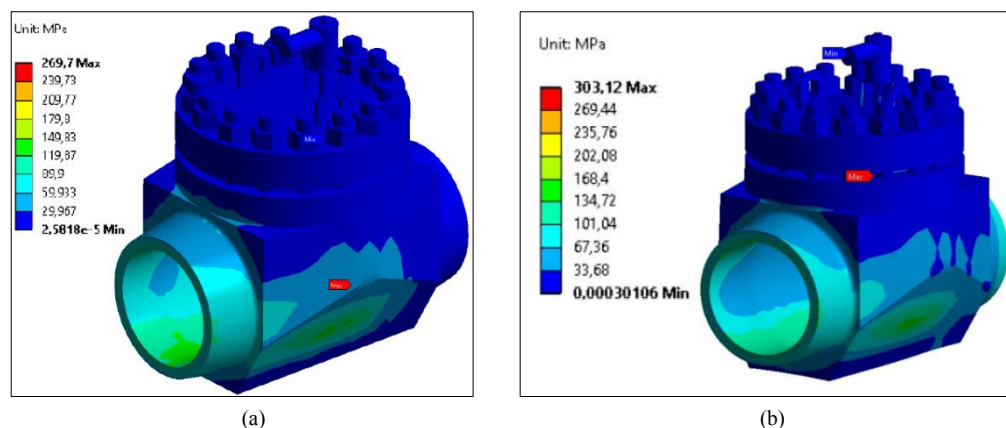


Figure 9. Distribution of equivalent stresses in the volume of the DN250 butterfly check valve at the minimum permissible temperature: a – cover closed; b – cover opened

Figure 10 shows graphical representations of the distribution of equivalent strains in the volumes of valve models at the maximum permissible temperature (45°C).

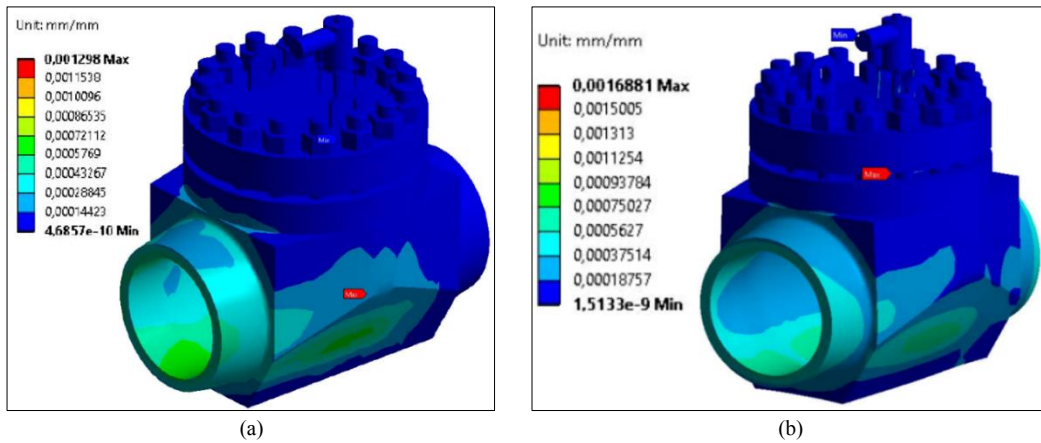


Figure 10. Distribution of equivalent strains in the volume of the DN250 butterfly check valve at the maximum permissible temperature: a – cover closed; b – cover opened

Figure 11 shows graphical representations of the distribution of equivalent strains in the volumes of the valve models at the minimum permissible temperature (-5°C).

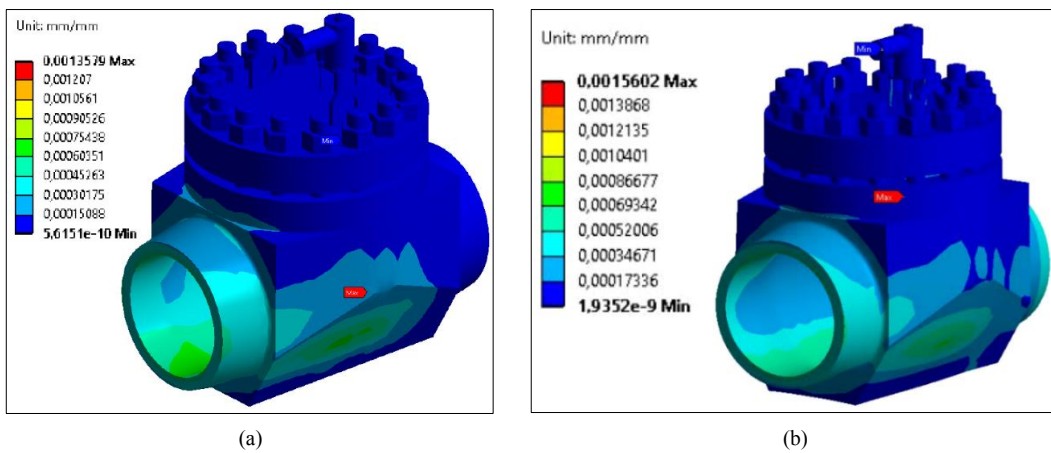


Figure 11. Distribution of equivalent strains in the volume of the DN250 butterfly check valve at the minimum permissible temperature: a – cover closed; b – cover opened

Figure 12 shows graphical representations of the distribution of equivalent displacements in the volumes of the valve models at the maximum permissible temperature (45°C)

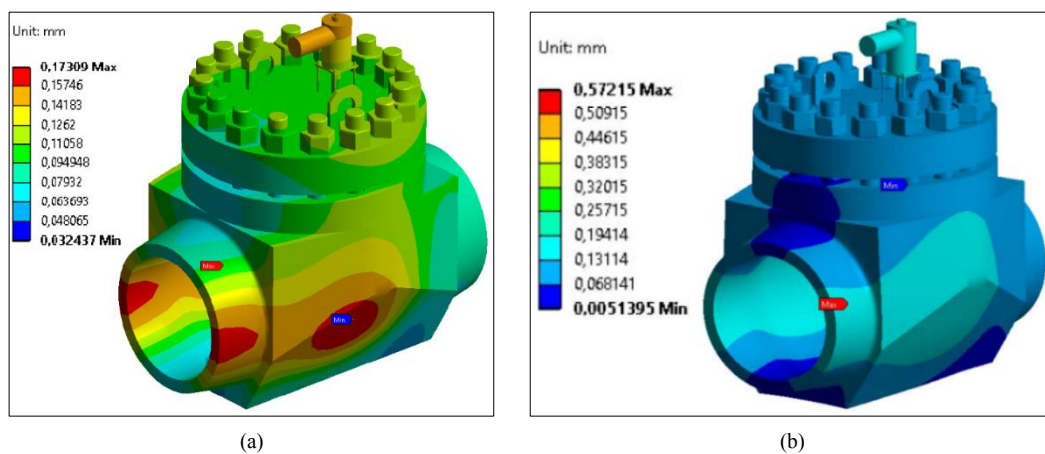


Figure 12. Distribution of equivalent displacements in the volume of the DN250 butterfly check valve at the maximum permissible temperature: a – cover closed; b – cover opened

Figure 13 shows graphical representations of the distribution of equivalent displacements in the volumes of the valve models at the minimum permissible temperature (-5°C).

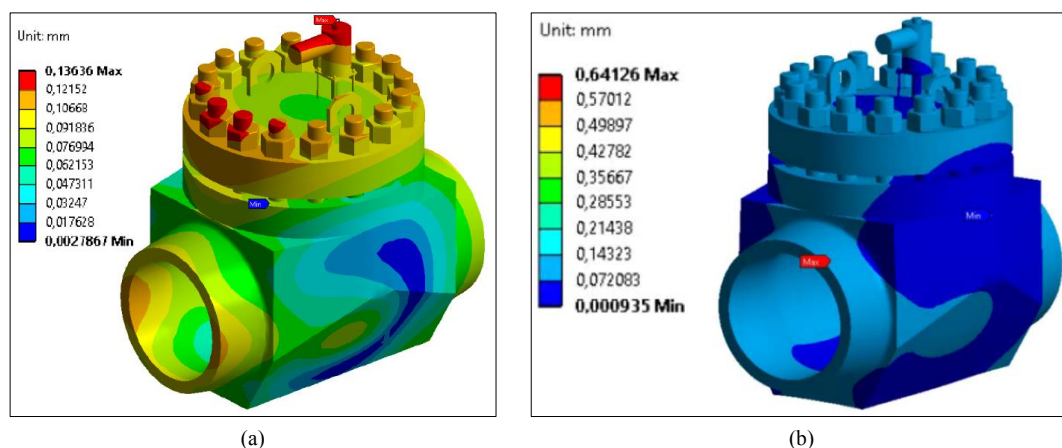


Figure 13. Distribution of equivalent displacements in the volume of the DN250 butterfly check valve at the minimum permissible temperature: a – cover closed; b – cover opened

The maximum values of equivalent stresses and strains under different conditions for the valve are achieved at a temperature of 45°C . The maximum value of displacements is achieved at a temperature of -5°C . These values correlate with the basic properties of steel [28] and the information given in Table 4, which shows that the lower the temperature, the greater the displacement for the X6CrNiTi18-10 alloy.

The obtained values are below the maximum permissible values for the selected material, which confirms the operability of the design being developed. Unlike the shutters of R.S. Collison, C.M. Engle, C.R. Hodny, and D.J. Koester described in the introduction, the developed design, according to the results of mathematical modeling, will withstand changes in ambient temperature.

5. Conclusion

This research made it possible to develop a BCV design and assess the stress-strain states of BCV components based on finite-element simulation techniques. The various materials used to manufacture the check valves involved in each piping system were reviewed. X6CrNiTi18-10 stainless steel grade was chosen for the manufacture of butterfly check valves because it has many advantages compared to C22 stainless steel grade: lower carbon content has a beneficial effect on anti-corrosion properties, and it has a larger temperature range for pumping media in aggressive environments. Some limitations were acknowledged in conducting this research. During the study, the 08X18H10T material was assigned, which is an analog of X6CrNiTi18-10. In addition, some limitations are indicated in the Methods and Materials section. The practical application of the developed BCV is its use in pipeline systems to ensure working fluid motion in a given direction and prevent it from moving in the opposite direction. BCV can also connect to horizontal and vertical sections of the pipeline.

Further research may be devoted to increasing the pipeline reliability in the area of connection with check valves, since crack-like defects intensively accumulate and develop in this area.

6. Declarations

6.1. Author Contributions

Conceptualization, J.S.; methodology, A.L.; software, A.L.; validation, A.K.; formal analysis, J.S.; investigation, A.L.; resources, A.K.; data curation, A.K.; writing—original draft preparation, A.L.; writing—review and editing, J.S.; visualization, A.L.; supervision, A.K.; project administration, A.L.; funding acquisition, A.L. All authors have read and agreed to the published version of the manuscript.

6.2. Data Availability Statement

The data presented in this study are available in the present article.

6.3. Funding

Some results of this research were obtained as part of the work under the Subsidy Agreement dated June 24, 2021 No. 075-11-2021-041 on the topic: “Development and commercialization of the butterfly check valves model range for pipeline systems of hazardous production facilities with ultra-high working parameters environment” with the Ministry of Science and Higher Education of the Russian Federation.

6.4. Conflicts of Interest

The authors declare no conflict of interest.

7. References

- [1] Fang, J., Cheng, X., Gai, H., Lin, S., & Lou, H. (2023). Development of machine learning algorithms for predicting internal corrosion of crude oil and natural gas pipelines. *Computers and Chemical Engineering*, 177, 108358. doi:10.1016/j.compchemeng.2023.108358.
- [2] Zheng, Q., Xu, Q., Shu, Z., Yang, D., Chen, W., Akkurt, N., Zhang, H., Lin, L., Zhang, X., & Ding, Y. (2023). A review of advances in mechanical behaviors of the underground energy transmission pipeline network under loads. *Gas Science and Engineering*, 117, 205074. doi:10.1016/j.jgsce.2023.205074.
- [3] Liu, M., Du, C., Luo, X., Liu, C., Wu, Z., & Li, X. (2023). Failure analysis in buried ductile iron pipelines: A study of leakage in drinking water distribution systems. *Engineering Failure Analysis*, 151, 107361. doi:10.1016/j.engfailanal.2023.107361.
- [4] Zhang, M., Guo, Y., Xie, Q., Zhang, Y., Wang, D., & Chen, J. (2022). Defect identification for oil and gas pipeline safety based on autonomous deep learning network. *Computer Communications*, 195, 14–26. doi:10.1016/j.comcom.2022.08.001.
- [5] Nakhal Akel, A. J., Paltrinieri, N., & Patriarca, R. (2022). Business analytics to advance industrial safety management. *Engineering Reliability and Risk Assessment*, 201–214. doi:10.1016/B978-0-323-91943-2.00006-X.
- [6] Lu, H., Xi, D., & Qin, G. (2023). Environmental risk of oil pipeline accidents. *Science of the Total Environment*, 874, 162386. doi:10.1016/j.scitotenv.2023.162386.
- [7] Yang, Y., Li, S., & Zhang, P. (2022). Data-driven accident consequence assessment on urban gas pipeline network based on machine learning. *Reliability Engineering and System Safety*, 219, 108216. doi:10.1016/j.res.2021.108216.
- [8] Ramírez-Camacho, J. G., Carbone, F., Pastor, E., Bubbico, R., & Casal, J. (2017). Assessing the consequences of pipeline accidents to support land-use planning. *Safety Science*, 97, 34–42. doi:10.1016/j.ssci.2016.01.021.
- [9] Zhang, W., Zhang, J. L., Li, X. J., Chen, F., Guo, J., Li, W., & Cai, J. (2022). Energy pipeline strength evaluation and reliability technology based on Fuzzy deep learning network algorithm. *Energy Reports*, 8, 5129–5136. doi:10.1016/j.egy.2022.03.203.
- [10] Alexandrov, I. A., Muranov, A. N., & Mikhailov, M. S. (2021). Development of an Algorithm for Automated Evaluation of the Operability of Structural Elements of Shut-off Valves. 2021 International Conference on Quality Management, Transport and Information Security, Information Technologies (IT & QM & IS), IEEE, Yaroslavl, Russian Federation. doi:10.1109/itqmis53292.2021.9642718.
- [11] Tatarkanov, A. A., Alexandrov, I. A., Mikhailov, M. S., & Muranov, A. N. (2021). Algorithmic Approach to the Assessment Automation of the Pipeline Shut-Off Valves Tightness. *International Journal of Engineering Trends and Technology*, 69(12), 147–162. doi:10.14445/22315381/IJETT-V69I12P218.
- [12] Mikhailov, M. S., Tatarkanov, A. A., Glashev, R. M., & Ivanov, N. Z. (2019). Actual Problems of Product Serviceability Assessment Based on the Analysis of Research Results Obtained Through X-Ray Computed Tomography Method. 2019 International Conference “Quality Management, Transport and Information Security, Information Technologies” (IT & QM & IS), Sochi, Russia. doi:10.1109/itqmis.2019.8928316.
- [13] Han, P., Hua, H., Wang, H., & Shang, J. (2023). A graphic partition method based on nodes learning for energy pipelines network simulation. *Energy*, 282, 128179. doi:10.1016/j.energy.2023.128179.
- [14] Towler, G., & Sinnott, R. (2022). Transport and storage of fluids. *Chemical Engineering Design*, 953–1001, Butterworth-Heinemann, Oxford, United Kingdom. doi:10.1016/b978-0-12-821179-3.00020-0.
- [15] Liu, T., Cheng, Y. F., Sharma, M., & Voordouw, G. (2017). Effect of fluid flow on biofilm formation and microbiologically influenced corrosion of pipelines in oilfield produced water. *Journal of Petroleum Science and Engineering*, 156, 451–459. doi:10.1016/j.petrol.2017.06.026.
- [16] Song, X., Yang, Y., Yu, D., Lan, G., Wang, Z., & Mou, X. (2016). Studies on the impact of fluid flow on the microbial corrosion behavior of product oil pipelines. *Journal of Petroleum Science and Engineering*, 146, 803–812. doi:10.1016/j.petrol.2016.07.035.
- [17] Calderón-Hernández, J. W., Sinatora, A., de Melo, H. G., Chaves, A. P., Mano, E. S., Leal Filho, L. S., Paiva, J. L., Braga, A. S., & Souza Pinto, T. C. (2020). Hydraulic convey of iron ore slurry: Pipeline wear and ore particle degradation in function of pumping time. *Wear*, 450–451, 203272. doi:10.1016/j.wear.2020.203272.
- [18] Brandt, M. J., Johnson, K. M., Elphinston, A. J., & Ratnayaka, D. D. (2017). Valves and Meters. *Twort’s Water Supply*, 743–775. doi:10.1016/b978-0-08-100025-0.00018-1.
- [19] Zheng, S., Luo, M., Xu, K., Li, X., Bie, Q., Liu, Y., Yang, H., & Liu, Z. (2019). Case study: Erosion of an axial flow regulating valve in a solid-gas pipe flow. *Wear*, 434–435, 202952. doi:10.1016/j.wear.2019.202952.

- [20] Chinyaev, I. R., Fominykh, A. V., & Ilinykh, E. A. (2016). The Valve is a Shutoff for the Passive Protection Systems of Pipelines. *Procedia Engineering*, 150, 220–224. doi:10.1016/j.proeng.2016.06.750.
- [21] Sotoodeh, K. (2021). Butterfly valve applications and design. In *A Practical Guide to Piping and Valves for the Oil and Gas Industry*, 147–241. doi:10.1016/b978-0-12-823796-0.00017-9.
- [22] Sotoodeh, K. (2021). Valve technology and selection. *A Practical Guide to Piping and Valves for the Oil and Gas Industry*, 559–584, Gulf Professional Publishing, Houston, United States. doi:10.1016/b978-0-12-823796-0.00021-0.
- [23] Collison, R. S., Engle, C. M., & Hodny, C. R. (2015). U.S. Patent No. 9,206,909. U.S. Patent and Trademark Office, Washington, United States.
- [24] Bazarov, A. A., Bondareva, N. V., & Navasardyan, A. A. (2022). Heating System for Rigid Wedge Valves. In *Proceedings of the 7th International Conference on Industrial Engineering (ICIE 2021) Volume 1(7)*, 21-31. doi:10.1007/978-3-030-54817-9_149.
- [25] Ghelloudj, O., Zelmati, D., Ramoul, C. E., Gharbi, A., Ayad, A., Aoun, I. D., Saadi, A., & Bachiri, A. (2023). Reliability assessment of pipeline steel under corrosion defect. *Materials Today: Proceedings*, 1-6. doi:10.1016/j.matpr.2023.05.212.
- [26] Li, X., Wang, J., Abbassi, R., & Chen, G. (2022). A risk assessment framework considering uncertainty for corrosion-induced natural gas pipeline accidents. *Journal of Loss Prevention in the Process Industries*, 75, 104718. doi:10.1016/j.jlp.2021.104718.
- [27] Vishnuvardhan, S., Murthy, A. R., & Choudhary, A. (2023). A review on pipeline failures, defects in pipelines and their assessment and fatigue life prediction methods. *International Journal of Pressure Vessels and Piping*, 201, 104853. doi:10.1016/j.ijpvp.2022.104853.
- [28] BS EN 10250-2:2000. (2000). Open die steel forgings for general engineering purposes -Part 2: Non-alloy quality and special Steels. British Standard Institute (BSI), London, United Kingdom.